

## Disorder-induced modification of the transmission of light through two-dimensional photonic crystals

This article has been downloaded from IOPscience. Please scroll down to see the full text article.

2005 J. Phys.: Condens. Matter 17 1781

(<http://iopscience.iop.org/0953-8984/17/12/002>)

View [the table of contents for this issue](#), or go to the [journal homepage](#) for more

Download details:

IP Address: 129.252.86.83

The article was downloaded on 27/05/2010 at 20:32

Please note that [terms and conditions apply](#).

## Disorder-induced modification of the transmission of light through two-dimensional photonic crystals

D M Beggs<sup>1,3</sup>, M A Kaliteevski<sup>1</sup>, R A Abram<sup>1</sup>, D Cassagne<sup>2</sup> and J P Albert<sup>2</sup>

<sup>1</sup> Department of Physics, University of Durham, South Road, Durham DH1 3LE, UK

<sup>2</sup> Groupe d'Etude des Semiconducteurs CC074, Université Montpellier II, Place Bataillon, 34095 Montpellier Cedex 05, France

E-mail: d.m.beggs@durham.ac.uk

Received 3 November 2004, in final form 18 January 2005

Published 11 March 2005

Online at [stacks.iop.org/JPhysCM/17/1781](http://stacks.iop.org/JPhysCM/17/1781)

### Abstract

Disordered two-dimensional photonic crystals with a complete photonic band-gap have been investigated. Transmission and reflection spectra have been modelled for both ballistic and scattered light. The density of states and electromagnetic field profiles of disorder-induced localized states have also been calculated, for various levels of disorder. It is found that there is a threshold-like behaviour in the amount of disorder. Below the threshold, it is seen that there is a vanishing probability of disorder-induced localized states being introduced into the centre of the photonic band-gap, but that edge-states narrow the band-gap. Above the threshold, there is a non-zero probability of disorder-induced localized states throughout the photonic band-gap, and the modification of the transmission and reflection spectra due to disorder rapidly increases with increasing disorder.

(Some figures in this article are in colour only in the electronic version)

Photonic crystals [1, 2] have attracted much attention over the last decade due to the ability to control light, and many potential applications have been identified. Many of the useful properties of photonic crystals derive from the existence of a photonic band-gap (PBG) that can result from the regular, periodic arrangement of dielectric material, where the period of the structure is of the order of the wavelength of the light. However, in reality, all photonic crystals will possess imperfections and hence a degree of disorder. For example, in self-organizing opal structures [3, 4] the spheres that make up the photonic crystal will have radii that fluctuate, and lattice vacancies will also be present. In 2D photonic crystals formed by etching air cylinders into a semiconductor substrate [1, 5–9], there are fluctuations in the cylinder radii, as well as

<sup>3</sup> Author to whom any correspondence should be addressed.

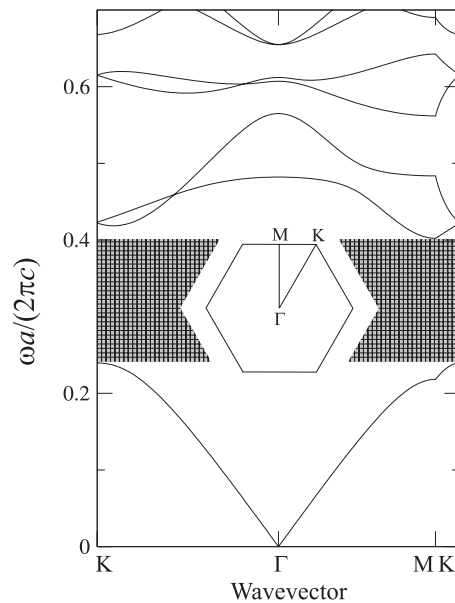


**Figure 1.** The calculated TE-polarized bandstructure for the ideal hexagonal lattice of air cylinders of radius  $0.4a$  embedded in a GaAs substrate ( $\epsilon = 12.96$ ). The hatched region indicates the complete 2D photonic band-gap for this structure. The first Brillouin zone of the ideal crystal is also shown (inset).

random shifts in the cylinder centres away from the ideal lattice points. Also, a certain surface roughness along the walls of the etched semiconductor will be present, and this introduces another form of disorder. Such disorder damages the band-gap by filling it with localized states, and could, in some cases, preclude the use of the photonic crystal in technological applications.

The present study aims to examine the effect of a certain type of disorder on the transmission and reflection spectra of a particular 2D photonic crystal with a complete PBG. The (ideal) photonic crystal is made up of air cylinders of radius  $0.4a$  (where  $a$  is the lattice constant, or separation of the centres of neighbouring cylinders) etched in a GaAs substrate ( $\epsilon = 12.96$ ), arranged in a hexagonal lattice. It possesses a wide, complete 2D PBG for the TE polarization (which has the electric field polarized in the plane of refractive index variation), and as such is well suited for this study. The bandstructure of the ideal crystal for this polarization, calculated using a plane wave method [6, 10, 11], is shown in figure 1. The disorder is of the form of a random shift of the individual cylinders away from their ideal lattice positions: the centre of the air cylinders in the disordered structure is located at a random position within a circle, centred on the ideal lattice points, of radius  $\delta a$ . Hence  $\delta$  is a measure of the ‘amount of disorder’.

This study follows on from previous work which looked at disorder in the same ideal structure [12, 13]. However, in [12] and [13] the disorder was of the form of a random change of the individual cylinder radii. Those studies found a threshold-like behaviour for the modification of the transmission spectra as a function of the ‘amount of disorder’; for small disorder the modification of the transmission spectra is small, but above the threshold amount of disorder the modification becomes large.

Experimentally, the transmission spectra of photonic crystals are studied in one of two ways. The ballistic transmission can be measured, where the transmitted light is in the

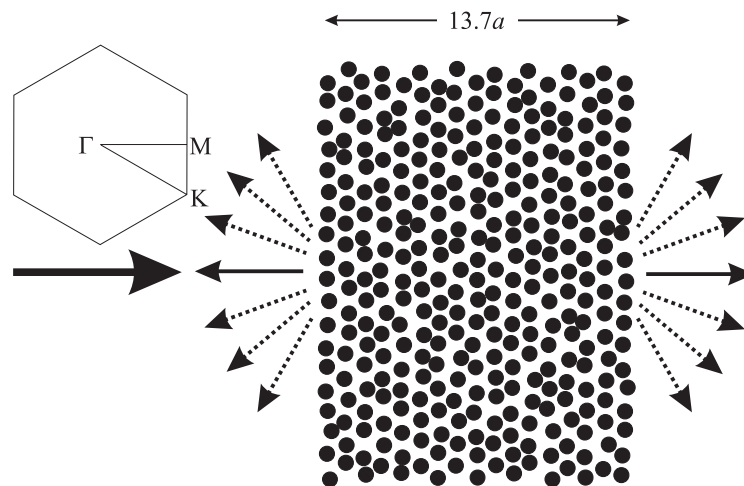


**Figure 2.** A schematic representation of the calculations undertaken. A disordered supercell is shown. The large arrow indicates the direction of incident light. The small solid arrows show the direction of ballistic transmission (right) and ballistic reflection (left). The dotted arrows indicate scattered transmission and reflection. Also shown is the first Brillouin zone of the ideal photonic crystal, which indicates the directions in reciprocal space.

same direction as the incident light; or the total transmission is measured, where all the light that emerges from the rear of the sample is collected, comprising the ballistic and scattered contributions. Hence in our modelling of the transmission spectra, we separately consider the ballistic and scattered transmission through the sample. Likewise for the reflection spectra, the total reflection is separated into contributions from the ballistic reflection (with an opposite direction to the incident wave) and scattered reflection. A schematic representation of the supercell used for the modelling of the spectra, and the definitions of ballistic and scattered reflection and transmission, are shown in figure 2.

Calculations of the spectra have been conducted using a combination of transfer matrix and multiple scattering methods, using a modified version of the publicly available code by Pendry *et al* [14–16]. Each cylinder was described by a 7 by 6 mesh, and periodic boundary conditions were imposed at the top and bottom sides of the structure. The sample thickness in the model was  $13.7a$ . The values of the deviation used in the modelling were  $\delta = 0.01, 0.02, 0.05, 0.1, 0.15$  and  $0.2$ , and for each case the transmission and reflection spectra were calculated for ten different random configurations of the disordered crystal. Figure 3 shows the calculated transmission and reflection spectra. The thin curves are the spectra for one individual configuration of disorder, shown as an example, and the thick curves are the mean spectra, averaged over all ten random configurations and additionally smoothed to remove the remaining traces of the spikes. The ballistic and scattered transmission and reflection are as per the figure caption. The ballistic transmission of the ideal crystal is also shown (as a dotted black curve) for comparison. The ideal crystal does not display any scattering of light, as the band-gap under study is below the diffraction cut-off of the crystal.

It can be seen from figure 3 that for small amounts of disorder ( $\delta \leq 0.05$ ) there is very little modification of the ballistic transmission relative to that for the ideal structure. For larger amounts of disorder, the modifications of the transmission spectra become rapidly more pronounced. For individual configurations of disorder, sharp spikes are present in the spectra, which correspond to localized states introduced into the PBG by the disorder. These sharp spikes then lead to an increase of the transmission on average in the region of the PBG where

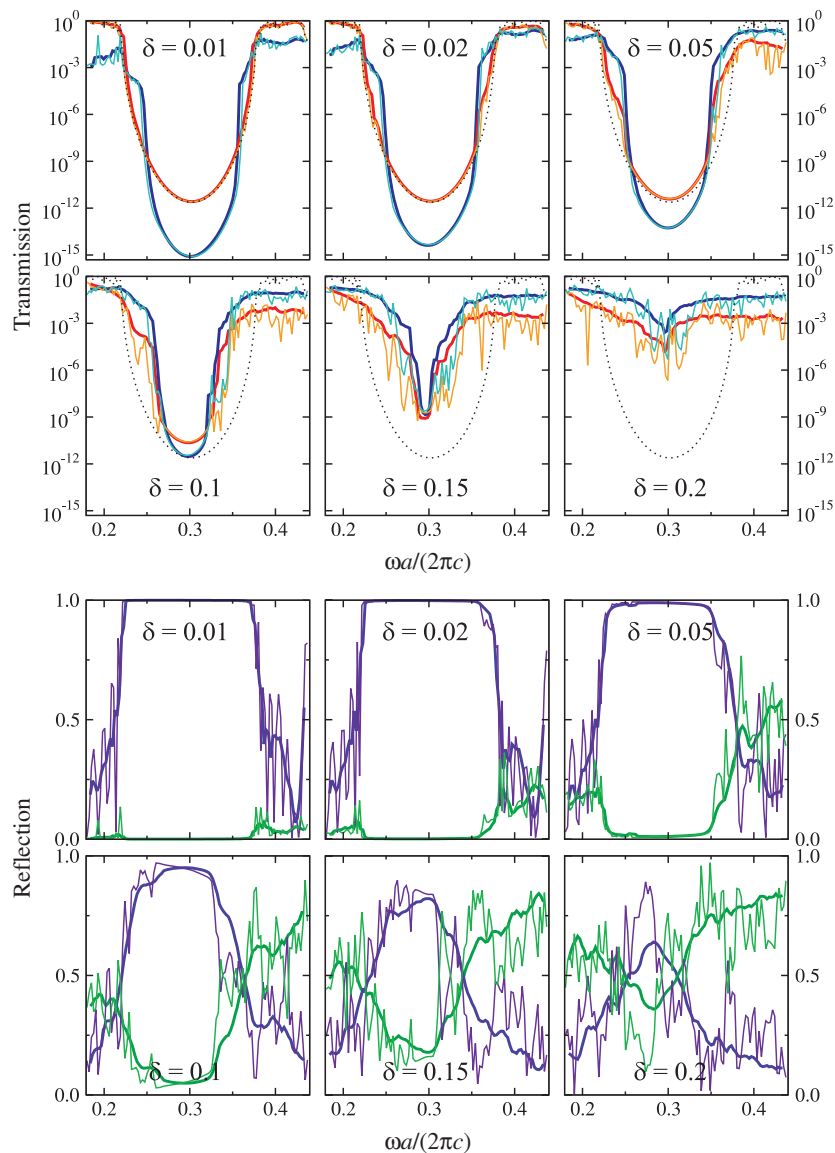


**Figure 3.** Top: calculated transmission spectra for disordered photonic crystals with  $\delta = 0.01, 0.02, 0.05, 0.1, 0.15$  and  $0.2$ . Solid (red) curves are the ballistic transmission, dashed (blue) curves are the scattered transmission—the thin curves for an individual configuration of disorder, and the heavy curves for the mean averaged over 10 random configurations of disorder. The ballistic transmission spectrum of the ideal photonic crystal is also shown (black dotted curve) for comparison. Bottom: calculated reflection spectra for the same structures. Solid (indigo) curves are the ballistic reflection, and dashed (green) curves are the scattered reflection.

they occur. Also the width of the ballistic transmission dip decreases with increasing disorder. This is due to the fact that small amounts of disorder can only introduce states into the PBG near its upper and lower edges (so-called edge-states) and thus act to narrow the band-gap of the photonic crystal. Only when the disorder becomes large can it introduce states into the centre of the PBG, and influence the transmission there. The transmission spectra of figure 3 also

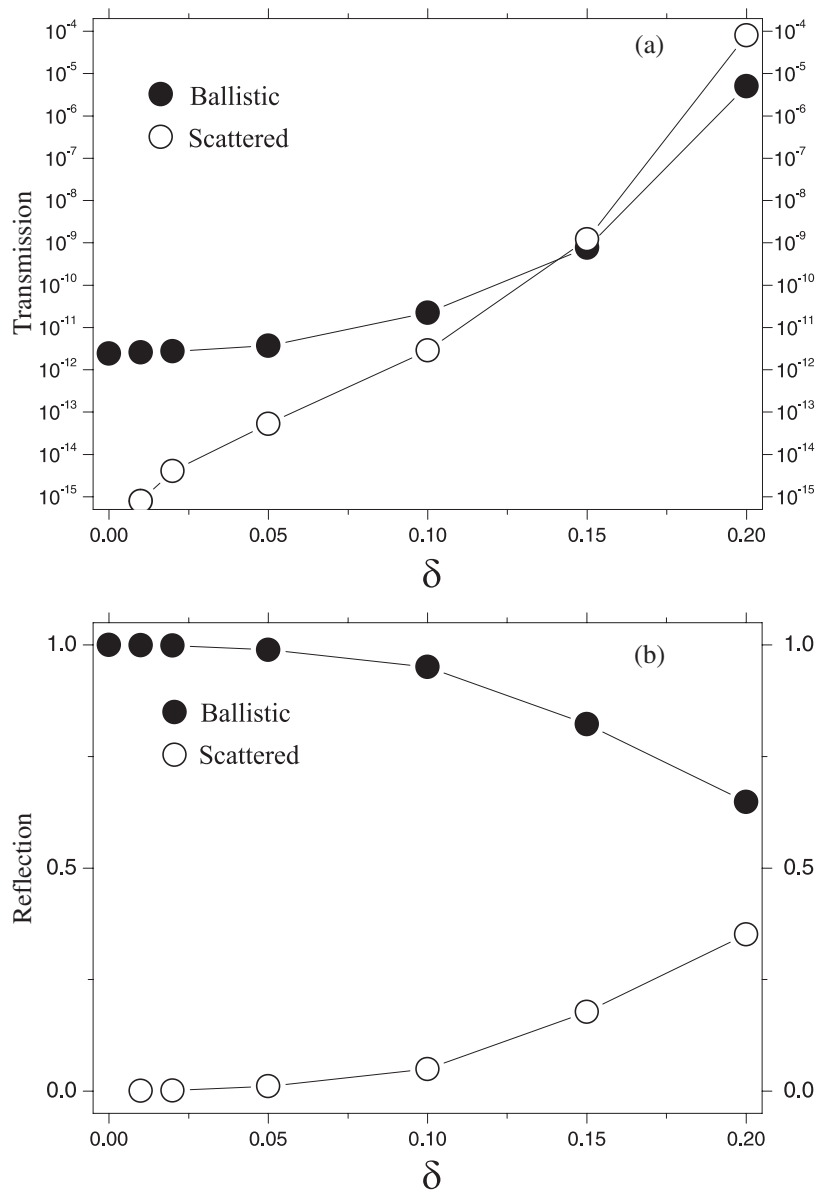


**Figure 4.** (a) The transmission coefficient at the minimum of the spectral dip for the averaged ballistic transmission (closed circles) and averaged scattered transmission (open circles) as a function of the 'amount of disorder',  $\delta$ . (b) The reflection coefficient at the spectral maximum for the averaged ballistic reflection (closed circles), and at the spectral minimum for the averaged scattered reflection (open circles) as a function of  $\delta$ .

show the calculated scattered transmission through the disordered supercells. For a relatively small amount of disorder ( $\delta = 0.01$ ), the scattered transmission in the transmission dip of the ideal photonic crystal is  $\sim 3$  orders of magnitude smaller than the ballistic transmission. Figure 4(a) shows the averaged transmission at the minimum as a function of the deviation  $\delta$  for both ballistic and scattered transmission. The different behaviour of the minimum transmission depending on the ballistic or scattered nature of the light is clear here. The ballistic transmission

is resistant to disorder up to some threshold value of  $\delta$ , after which it increases rapidly. The scattered transmission increases rapidly with  $\delta$  even for small values  $\delta$ . Moreover, the scattered transmission increases with  $\delta$  at a faster rate than the ballistic transmission does, so that for large value of the disorder parameter, scattered light is dominant in the transmission spectrum. These results are qualitatively similar to results obtained in [13], which presented the effect of disorder in the form of chaotic cylinder radii on the transmission spectra.

Also present in the transmission spectra is an effect attributed to Rayleigh scattering. The ballistic transmission on the upper frequency edge of the transmission dip is smaller than that on the lower edge when disorder is present. This is because the Rayleigh scattering due to disorder, which removes light from the ballistic transmission, is stronger at the higher frequencies.

The bottom of figure 3 shows the reflection spectrum calculated for  $\delta = 0.01, 0.02, 0.05, 0.1, 0.15$  and  $0.2$ . Again it can be seen that, for small disorder, the scattered reflection remains very small, and in the region of the ideal crystal's photonic band-gap the ballistic reflection is close to unity. Upon increasing the amount of disorder, the averaged scattered reflection begins to grow. For  $\delta \geq 0.1$ , this growth increases in rate (see figure 4(b)). The decline of the averaged ballistic reflection with increasing  $\delta$  mirrors the rise of the scattered reflection. Also, once again, the effect of Rayleigh scattering can be seen, as the averaged scattered reflection on the upper frequency edge of the PBG is greater than that of the lower frequency edge, and the onset of significant amounts of scattered reflection occurs at a lower value of  $\delta$  for the upper frequency edge.

When light is incident upon a finite photonic crystal, attenuation of the light occurs in the spectral region of the infinite crystal's PBG, and a transmission dip (such as is shown by the transmission spectra of figure 3) is observed. In the photonic crystal under consideration, the transmission coefficient decays exponentially with an increase of path length through the crystal for both ballistic and scattered light. An attenuation length,  $\xi$ , can be defined using the ballistic transmission coefficient through the structure,  $T_B$ , as

$$T_B = \exp(-L/\xi) \quad (1)$$

where  $L$  is the thickness of the sample, which, in the modelling undertaken is  $L = 13.7a$ . Figure 5 shows the mean and standard deviation of the attenuation length at the centre of the PBG as a function of the deviation  $\delta$ , and the insets show the attenuation lengths as a function of frequency for different values of  $\delta$ . As the disorder in the photonic crystals increases, the mean attenuation length rises. For the ideal crystal, at a frequency corresponding to the centre of the photonic band-gap, the attenuation length is  $0.51a$ . Small amounts of disorder ( $\delta \leq 0.1$ ) have very little effect on the attenuation length at the centre of the PBG. When  $\delta = 0.1$ , the attenuation length has reached  $0.56a$ , which is only a 10% increase on the ideal value. However, for larger amounts of disorder ( $\delta \geq 0.15$ ), the rate of increase of the attenuation length increases, and for  $\delta = 0.2$  the attenuation length at the centre of the PBG is  $1.1a$ , a 110% increase on the ideal value. Also, for small disorder ( $\delta \leq 0.1$ ), the standard deviation of the attenuation length at the centre of the PBG is very close to zero ( $\sim 10^{-4}$ ), implying that it is very unlikely that any disorder-induced localized states will penetrate to the centre of the band-gap and affect the attenuation length there. As the value of  $\delta$  increases, the standard deviation of the attenuation length at the centre of the PBG begins to rise rapidly, suggesting that it is more probable for a disorder-induced localized state to be present at the centre of the PBG.

Figure 6 shows the calculated density of states (DOS), averaged over ten random configurations of disorder for each of the values  $\delta = 0.05, 0.1, 0.15$  and  $0.2$ . The calculations were performed by a plane wave method, using a rectangular supercell of 93 air cylinders arranged in a hexagonal lattice with disorder imposed upon the system. Periodic boundary

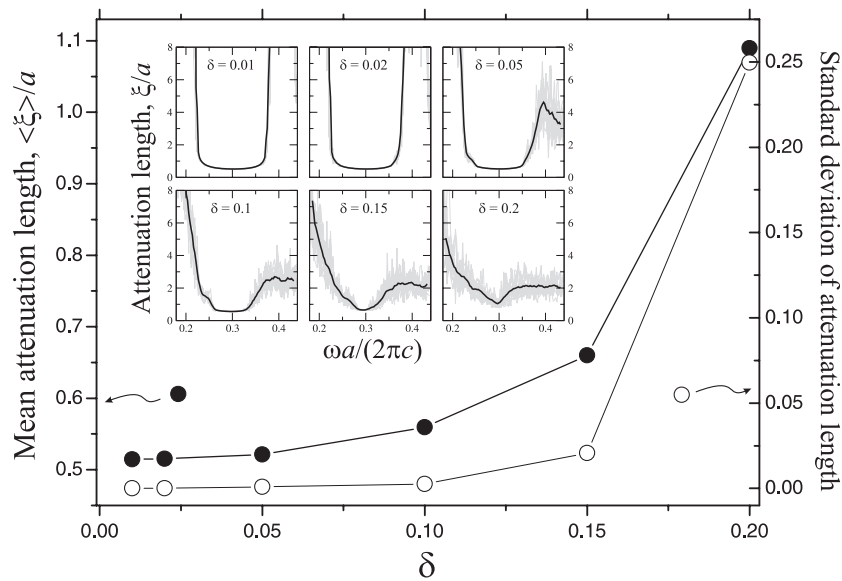


**Figure 5.** The mean attenuation length (closed circles, left axis) and its standard deviation (open circles, right axis) at the centre of the ideal crystal's photonic band-gap as a function of  $\delta$ . Inset: the spectra of the attenuation lengths for  $\delta = 0.01, 0.02, 0.05, 0.1, 0.15$  and  $0.2$ . Black curves are the mean over the ten random configurations, and grey curves are the ten individual configurations.

conditions were assumed, and the eigenfrequencies of the super-crystal were calculated at the  $\Gamma$ -point in reciprocal space. A basis set of 6561 plane waves was used for the calculation. When performed with no disorder, the calculation gives the band-gap to be between  $\omega a / (2\pi c) = 0.25$  and  $0.43$ , which indicates convergence to approximately 6% at frequencies corresponding to the PBG of the ideal crystal. From figure 6, it can be seen how edge-states are introduced into the PBG for small amounts of disorder ( $\delta = 0.05$  and  $0.1$ ), but these states are confined to a spectral region near the edge of the PBG—i.e. there is a vanishing probability for a localized state to be introduced into the centre of the PBG. It is these edge states which cause the narrowing of the PBG, which is manifested in the spectra of figure 3. Also note how states are introduced into the upper portion of the PBG much more readily than the lower, so that for small disorder the states from the upper band penetrate the gap more deeply than those from the lower band. At the threshold amount of disorder, the probability of disorder-induced localized states being introduced into the centre of the former PBG becomes non-zero. Hence localized states also have a non-zero probability of appearing anywhere in the PBG. It is these localized states that produce the sharp spikes in the transmission dip of the disordered photonic crystals, and which leads to the raising of the level of configuration averaged transmission.

Figure 7 shows the magnetic field profiles for the deepest lying state in the former PBG for a particular configuration of disorder for the values  $\delta = 0.05, 0.1, 0.15$  and  $0.2$ . The magnetic field profiles are shown, as the magnetic field for the TE polarization is perpendicular to the plane of refractive index variation, and so is easier to visualize than the electric field, which lies in the plane and varies in direction as well as magnitude. As the amount of disorder is increased, localized states are introduced deeper into the former PBG of the ideal crystal (see figure 6).

Strictly speaking, the plane-wave calculations give the eigenfrequencies of an artificial rectangular lattice of the same disordered supercell. Thus we must ensure that the supercell is



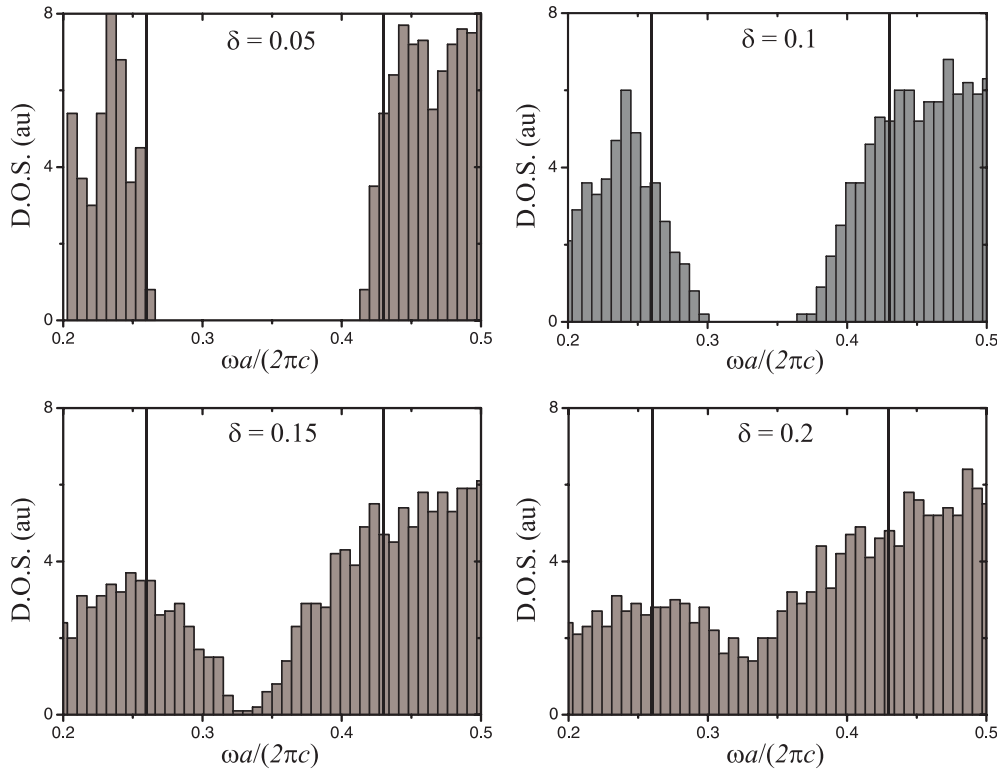


**Figure 6.** Density of states (DOS) averaged over ten random configurations of disorder for the values  $\delta = 0.05, 0.1, 0.15$  and  $0.2$ . The vertical black lines show the upper and lower edges of the PBG of the ideal photonic crystal.

large enough for the super-crystalline nature to be a good representation of an infinite, randomly disordered structure. However, we must also ensure that the calculations are converged to a reasonable accuracy, and so the computational cost limits the size of the supercell that can be used. The calculation produces mini-bands of disorder-induced localized states within the ideal photonic crystal's PBG. The width of the mini-bands is physically due to the diffusion of photons between localization sites within the super-crystal, and so will depend upon the spatial overlap of the states and thus on the size of the supercell used. Thus, when we consider the system as large enough to ignore its super-crystalline nature, the width of each mini-band gives a rough estimate of the reciprocal lifetime of the localized state. Dispersion curves of the localized states shown in figure 7 have been calculated, and indeed mini-bands are seen. However, the mini-bands are very narrow, and show very little dispersion, and are not presented in this paper. For the states shown in figure 7, the widths of the mini-bands ( $\Delta\omega$ ) relative to their centre frequencies ( $\omega_0$ ) are as follows. The  $\delta = 0.05$  state has  $\omega_0 a / (2\pi c) = 0.26$  and  $\Delta\omega / \omega_0 = 0.5\%$ ; the  $\delta = 0.1$  state has  $\omega_0 a / (2\pi c) = 0.29$  and  $\Delta\omega / \omega_0 = 0.02\%$ ; the  $\delta = 0.15$  state has  $\omega_0 a / (2\pi c) = 0.32$  and  $\Delta\omega / \omega_0 = 0.03\%$ ; and the  $\delta = 0.2$  state has  $\omega_0 a / (2\pi c) = 0.34$  and  $\Delta\omega / \omega_0 = 0.06\%$ . This confirms what can already be seen from an inspection of the field profiles of figure 7: that the weakly bound state for  $\delta = 0.05$  is delocalized, whereas the other deeper lying states are essentially localized.

In conclusion, the effect of disorder on the spectra of two-dimensional photonic crystals composed of air cylinders in a GaAs substrate has been investigated. The disorder is of the

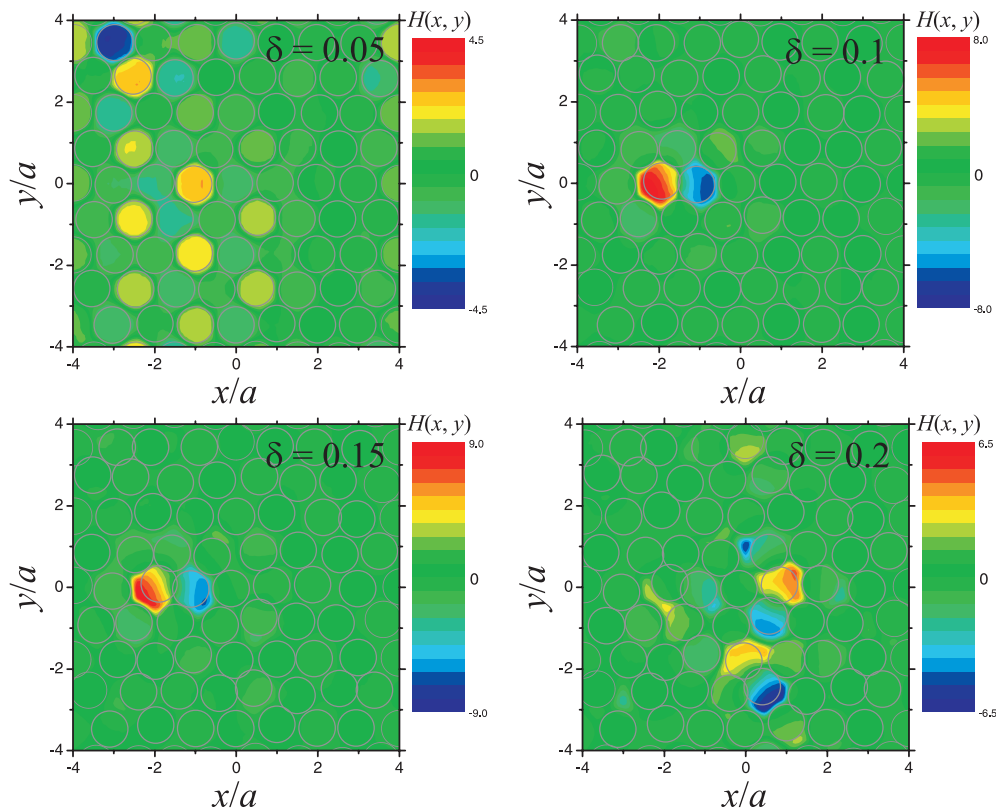


**Figure 7.** Magnetic field profiles calculated using a plane wave method. The field profiles shown are for a particular configuration of disorder, and represent the deepest lying disorder-induced state within the lower portion of the photonic band-gap. The frequencies are as follows:  $\delta = 0.05$ ,  $\omega_0 a / (2\pi c) = 0.26$ ;  $\omega_0 a / (2\pi c) = 0.29$ ;  $\delta = 0.15$ ,  $\omega_0 a / (2\pi c) = 0.32$ ; and  $\delta = 0.2$ ,  $\omega_0 a / (2\pi c) = 0.34$ .

form of a random shift of the air cylinders away from their ideal lattice locations. It was found that for a small amount of disorder there is a vanishing probability of disorder-induced localized states appearing in the centre of the former PBG, but the PBG of the disordered crystal narrows due to the introduction of edge-states. A threshold amount of disorder was found to exist, where the probability of finding disorder-induced localized states throughout the former PBG becomes non-zero. After this threshold, increasing the disorder has a significant effect on the spectra throughout the former PBG.

### Acknowledgment

This work was funded by an ESPRC research grant.

### References

- [1] Joannopoulos J D, Meade R D and Winn J N 1995 *Photonic Crystals: Molding the Flow of Light* (Princeton, NJ: Princeton University Press)
- [2] Sakoda K 2001 *Optical Properties of Photonic Crystals* (Berlin: Springer) (ISBN: 3-540-41199-2)
- [3] Vlasov Y A, Kalitevski M A and Nikolaev V V 1999 *Phys. Rev. B* **60** 1555

- [4] Blanco A, Chomski E, Grabtchak S, Ibisate M, John S, Leonard S W, Lopez C, Meseguer F, Miguez H, Mondia J P, Ozin G A, Toader O and van Driel H M 2000 *Nature* **405** 437
- [5] Winn J N, Meade R D and Joannopoulos J D 1994 *J. Mod. Opt.* **41** 257
- [6] Plihal M and Maradudin A A 1991 *Phys. Rev. B* **44** 8565
- [7] Yablonovich E 1993 *J. Phys.: Condens. Matter* **5** 2443
- [8] Pacradouni V, Mandeville W J, Cowan A R, Paddon P, Young J F and Johnson S R 2000 *Phys. Rev. B* **62** 4204
- [9] Zelsmann M, Picard E, Charvolin T, Hadji E, Heitzmann M, Dal'zotto B, Nier M E, Seassal C, Rojo-Romeo P and Letartre X 2003 *Appl. Phys. Lett.* **83** 2542–4
- [10] Ho K M, Chan C T and Soukoulis C M 1990 *Phys. Rev. Lett.* **65** 3152
- [11] Meade R D, Brommer K D, Rappe A M and Joannopoulos J D 1992 *Appl. Phys. Lett.* **61** 495
- [12] Kaliteevski M A, Manzanares Martinez J, Cassagne D and Albert J P 2002 *Phys. Rev. B* **66** 113101
- [13] Kaliteevski M A, Manzanares Martinez J, Cassagne D and Albert J P 2003 *Phys. Status Solidi a* **195** 612–7
- [14] Pendry J B and MacKinnon A 1992 *Phys. Rev. Lett.* **69** 2772
- [15] Pendry J B 1994 *J. Mod. Opt.* **41** 209–29
- [16] Bell P M, Pendry J B, Martin Moreno L and Ward A J 1995 *Comput. Phys. Commun.* **85** 306–22